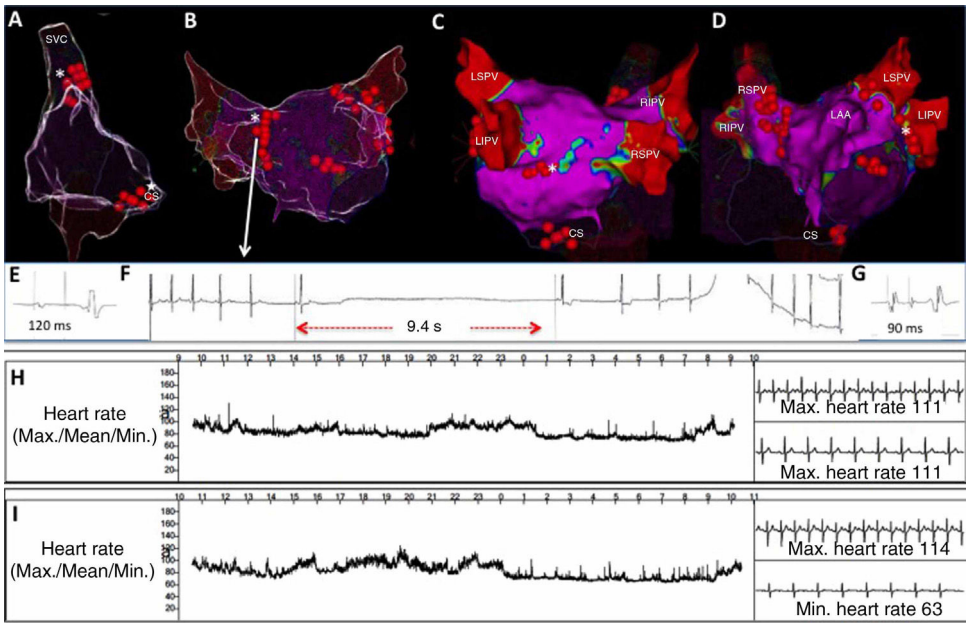

Figure 2. A: anatomical reconstruction of the right atrium (RA) showing the radiofrequency applications at the junction of the superior vena cava (SVC) with the RA (asterisk) and at the coronary sinus (CS) ostium (star). B: anterior view of the left atrium mainly showing the lesions contralateral to the SVC in the anterosuperior region of the right pulmonary vein (asterisk). C: posterior view of the left atrium showing the 4 pulmonary veins (PVs): left superior (LSPV), left inferior (LIPV), right superior (RSPV), and right inferior (RIPV). D: anterior view (slightly oriented toward the left) showing the applications in the region of the ridge between the left atrial appendage (LAA) and the left PVs (asterisk). E: AH interval before ablation. F: asystole provoked by radiofrequency application in the anterosuperior region of the RSPV. G: AH interval after ablation. H and I: Holter-ECG frequency histograms obtained 1 and 4 months after ablation.

Moisés Rodríguez-Mañero,[a,b,c,*] José Luis Martínez-Sande,[a,b,c] Laila González-Melchor,[a] Javier García-Seara,[a] Inés Gómez Otero,[a] and José Ramón González-Juanatey[a,b,c]

[a]*Departamento de Cardiología, Complejo Hospital Universitario de Santiago, Santiago de Compostela, A Coruña, Spain*
[b]*Instituto de Investigación Sanitaria (IDIS), Universidad de Santiago de Compostela, Santiago de Compostela, A Coruña, Spain*
[c]*Centro de Investigación Biomédica en Red de Enfermedades Cardiovasculares (CIBERCV CB16/11/00226 - CB16/11/00420), Santiago de Compostela, A Coruña, Spain*

*Corresponding author:
E-mail address: moirmanero@gmail.com (M. Rodríguez-Mañero).

Available online 26 June 2020

REFERENCES

1. Qin M, Zhang Y, Liu X, et al. Atrial ganglionated plexus modification: a novel approach to treat symptomatic sinus bradycardia. *JACC Clin Electrophysiol.* 2017;3:950–959.
2. Debruyne P, Rossenbacker T, Collienne C, et al. Unifocal right-sided ablation treatment for neurally mediated syncope and functional sinus node dysfunction under computed tomographic guidance. *Circ Arrhythm Electrophysiol.* 2018;11:e006604.
3. Brignole M, Donateo P, Tomaino M, et al. Benefit of pacemaker therapy in patients with presumed neurally mediated syncope and documented asystole is greater when tilt test is negative: an analysis from the third International Study on Syncope of Uncertain Etiology (ISSUE-3). *Circ Arrhythm Electrophysiol.* 2014;7:10–16.
4. Brignole M, Moya A, de Lange FJ, et al.ESC Scientific Document Group. 2018 ESC Guidelines for the diagnosis and management of syncope. *Eur Heart J.* 2018;39:1883–1948.

https://doi.org/10.1016/j.rec.2020.04.019
1885-5857/

Left ventricle myocardial deformation pattern in severe aortic valve stenosis without cardiac amyloidosis. The AMY-TAVI trial

Patrón de deformación miocárdica del ventrículo izquierdo en la estenosis aórtica grave sin amiloidosis cardiaca. Estudio AMY-TAVI

To the Editor,

Cardiac amyloidosis (CA) is characterized by extracellular deposition of amyloid fibrils in the myocardium and other cardiac structures. Although its actual prevalence is unknown, transthyretin-related CA is thought to be present in 15% to 30% of patients with aortic stenosis (AS) treated by transcatheter aortic valve implantation (TAVI), possibly identifying a patient subgroup with a poorer prognosis. Echocardiography is an essential tool used to establish the initial diagnostic suspicion. However, the coexistence of AS and CA could mask the diagnosis of the latter, as they share common features.[1]

Several publications report on advanced echocardiographic indices based on left ventricular longitudinal myocardial strain, which could differentiate CA from other forms of hypertrophy. These indices include RELAPS (relative apical sparing of longitudinal strain [LS]),[2] septal apical to basal LS ratio (SAB),[3] or left ventricular ejection fraction (LVEF) to global longitudinal strain (GLS) ratio (EFSR).[4]

Our aim was to assess the diagnostic utility of applying these LS-based echocardiographic criteria described for suspected CA in patients with severe AS without amyloidosis.

As part of the AMY-TAVI (NCT03984877) trial to study the prognostic impact of CA in patients with severe AS who

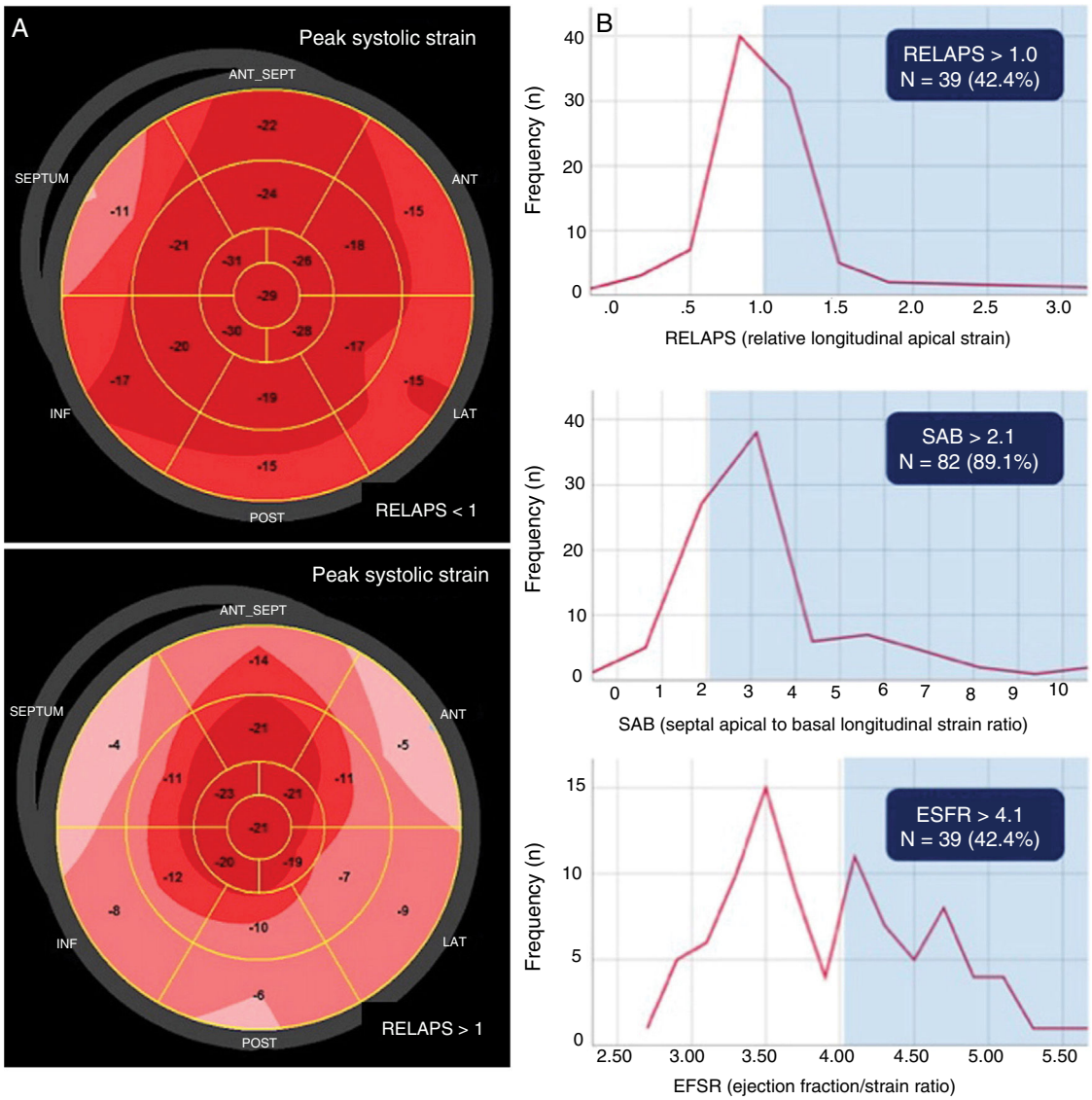

Figure 1. A, LS phenotypes in the polar map in severe AS according to the RELAPS value. The RELAPS > 1 pattern represents normal apical strain. B, patients with severe and symptomatic AS and myocardial strain indices within the range indicating CA (n = 92). Patient distribution according to RELAPS, SAB, and EFSR values. AS, aortic stenosis; CA, cardiac amyloidosis; EFSR, ejection fraction to strain ratio; LS, longitudinal strain; RELAPS, relative apical sparing of longitudinal strain; SAB, septal apical to basal longitudinal strain ratio.

underwent TAVI, 109 consecutive patients were prospectively included between January and August 2019 if they had a diagnosis of severe symptomatic AS without CA and had an indication for TAVI. Pre-procedure echocardiography included conventional parameters and myocardial deformation parameters on speckle-tracking echocardiography (2DSTE); these parameters were only measured in 92 patients, due to a poor acoustic window that caused inadequate tracking in the remaining 17 patients. The same expert operator obtained all echocardiograms (blinded) using a Vivid E95 unit, and all echocardiograms were analyzed offline with the EchoPAC Clinical Workstation v202 Software (GE Healthcare, Norway). Polar maps were acquired by AFI algorithms with quantitative information from the LS generated from the 3 apical planes, with a frame rate of 50 to 80 cps, and were divided into 17 segments. Strain was averaged using 6 basal, 6 medial, and 4 apical segments (excluding segment 17). The relative apical LS was calculated using the formula: RELAPS = average apical LS / average basal SL + average mid LS. According to the literature,[2] RELAPS > 1 indicates CA, with the polar map showing a bright red pattern in the apical segments and more pinkish pattern in the basal and mid-ventricular segments (figure 1A). The SAB ratio was calculated as the septal apical to basal LS ratio, and it was considered that a value > 2.1 indicated CA.[3] The EFSR ratio was calculated as LVEF over GLS. The cutoff point for CA was established as 4.1.[4]

Post-TAVI ^{99}Tc pyrophosphate scintigraphy and serum protein electrophoresis were performed for CA screening, and patients with a positive result were excluded.

Categorical variables are expressed as frequencies and percentages, and continuous variables are expressed as the mean ± standard deviation. Qualitative variables were compared using the chi squared test, and continuous variables were compared using the Student *t* test for independent samples. To identify predictive factors of an apical sparing pattern (RELAPS > 1), a logistic regression model was constructed by the backward stepwise selection method using maximum likelihood estimates, including any variables that were statistically significant or had $P < .1$ in the bivariate analysis. The odds ratio (OR) and 95% confidence intervals (95%CI) were calculated. A P value < .05 was considered significant. All data were analyzed using SPSS ver. 25.

Table 1
Patient characteristics according to systolic strain phenotype in the polar map

Clinical, demographic, and echocardiography parameters	Overall population (n = 92)	RELAPS < 1 (n = 53)	RELAPS > 1 (n = 39)	*P*
Demographic variables				
Age, y	82.1 ± 5.2	82.4 ± 5.4	81.7 ± 4.9	.492
Women	54 (58.7)	29 (54.7%)	25 (64.1%)	.366
BMI	29.1 ± 5.8	29.6 ± 6.4	28.4 ± 4.7	.296
Cardiovascular risk factors				
HTN	76 (82.6)	45 (84.9%)	31 (79.5%)	.498
DL	64 (69.6)	34 (64.2%)	30 (76.9%)	.233
DM	28 (30.4)	14 (26.4%)	14 (35.9%)	.329
Cardiovascular disease				
Prior MI	8 (8.7)	6 (11.5)	2 (5.1)	.285
Prior HF	33 (35.9)	21 (39.6%)	12 (30.8%)	.382
NYHA				.203
II	22 (23.9)	9 (17.0)	13 (33.3)	
III	64 (69.6)	39 (73.6)	25 (67.6)	
IV	6 (6.5)	5 (9.4)	1 (2.7)	
AF	26 (28.3)	13 (24.5%)	13 (33.3%)	.354
Peripheral artery disease	10 (10.9)	6 (11.3)	4 (10.3)	.871
Stroke	10 (10.9)	4 (7.5)	6 (15.4)	.233
Comorbidity				
CKF	17 (18.5)	12 (22.6%)	5 (12.8)	.230
Anemia	58 (63)	36 (67.9%)	22 (56.4%)	.258
COPD	10 (10.9)	7 (13.2)	3 (7.7)	.401
Prior neoplasm	14 (15.2)	8 (15.1)	6 (15.4)	.969
Conventional morphology parameters				
IVSd, mm	15.0 ± 2.9	14.2 ± 2.8	16.2 ± 3.0	.001
PWTd, mm	13.0 ± 2.1	12.5 ± 2.1	13.8 ± 1.8	.004
LV mass, g	303.5 ± 69.2	288.8 ± 66.4	323.3 ± 68.7	.018
LV mass index, g/m^2	178.6 ± 41.2	168.2 ± 39.2	192.48 ± 40.1	.005
LVEDD, mm	50.5 ± 6.1	51.2 ± 6.4	49.5 ± 5.7	.190
LVEDV, mL	103.0 ± 36.3	112.1 ± 37.8	90.7 ± 30.5	.005
LVESV, mL	47.2 ± 31.7	53.9 ± 34.8	38.2 ± 24.2	.012
ECC IND	1.2 ± 0.2	1.1 ± 0.2	1.2 ± 0.2	.353
MWT, mm	15.1 ± 2.8	14.3 ± 2.6	16.1 ± 2.7	.003
RWT, mm	0.5 ± 0.1	0.5 ± 0.1	0.6 ± 0.1	.008
LAVi, mL/m^2	58.2 ± 20.9	55.2 ± 17.1	63.0 ± 24.6	.223
Systolic function parameters				
LVEF, %	57.6 ± 15.2	55.3 ± 16.6	60.7 ± 12.8	.096
MAPSE, mm	12.0 ± 2.7	12.2 ± 2.9	11.7 ± 2.6	.433
S'	6.3 ± 1.7	6.5 ± 1.8	6.2 ± 1.7	.468
MCF	0.20 ± 0.07	0.22 ± 0.07	0.18 ± 0.05	.001
Diastolic function parameters				
E wave	95.8 ± 32.9	96.3 ± 31.7	95.1 ± 34.8	.860
E/E'	19.7 ± 7.9	18.8 ± 6.5	20.9 ± 9.2	.213
DT, ms	264.2 ± 112.7	240.8 ± 113.0	297.0 ± 105.0	.030
Myocardial deformation parameters				
GLS	−15.1 ± 4.8	−15.2 ± 5.4	−14.9 ± 3.8	.979
Basal LS	−9.5 ± 3.9	−10.9 ± 3.5	−7.6 ± 3.5	< .001
Mid LS	−13.5 ± 4.7	−14.1 ± 5.5	−12.6 ± 3.5	.109
Apical LS	−21.5 ± 8.5	−19.7 ± 9.7	−23.9 ± 5.9	.012
Aortic valve disease parameters				
AVA, cm^2	0.6 ± 0.1	0.7 ± 0.1	0.6 ± 0.1	.041
V_{max}, m/s	4.5 ± 0.6	4.4 ± 0.5	4.7 ± 0.6	.018
AVG_{max}, mmHg	85.3 ± 21.6	80.9 ± 18.6	91.4 ± 24.1	.021

Table 1 *(Continued)*
Patient characteristics according to systolic strain phenotype in the polar map

Clinical, demographic, and echocardiography parameters	Overall population (n = 92)	RELAPS < 1 (n = 53)	RELAPS > 1 (n = 39)	*P*
AVG_{mean}, *mmHg*	51.9 ± 14.2	48.9 ± 13.2	55.9 ± 14.9	.020
AET, ms	333.3 ± 37.5	340.2 ± 38.0	324.4 ± 35.3	.053

AET, aortic ejection time; AF, atrial fibrillation; apical LS, average peak systolic longitudinal strain of the apical segments; AVG_{max}, peak aortic valve gradient; AVG_{mean}, mean aortic valve gradient; AVA, aortic valve area; basal LS, average peak systolic longitudinal strain of the basal segments; BMI, body mass index; CKF, chronic kidney failure; COPD, chronic obstructive pulmonary disease; DL, dyslipidemia; DM, diabetes mellitus; DT, E-wave transmitral deceleration time; E/E', ratio of early mitral inflow E-wave to pulsed-wave tissue Doppler mitral annular E' wave; ECC IND, eccentricity index (IVSd/PWTd ratio); GLS, global longitudinal strain; HF, prior admission due to heart failure; HTN, hypertension; IVSd, interventricular septal thickness at end diastole; LAVi, indexed left atrial volume by biplane area-length method; LVEDD, LV end-diastolic diameter; LVEDV, LV end-diastolic volume; LVESV, LV end-systolic volume; MCF, myocardial contraction fraction (ratio of stroke to myocardial volume, ie, LV mass ratio/1.05) (myocardial density); mid LS, average peak systolic longitudinal strain of the medial segments; MI, history of myocardial infarction; MWT, maximum wall thickness; PWTd, posterior wall thickness at end diastole; RWT, relative wall thickness (2×PWT/LVEDD); S', S' wave of the lateral mitral annulus with pulsed-wave tissue Doppler; stroke, history of ischemic stroke; V_{max}, peak aortic jet velocity.
Data are expressed as No. (%) or mean ± standard deviation.

Table 1 lists the baseline characteristics of the entire cohort analyzed with myocardial deformation parameters and the differences between the RELAPS < 1 and > 1 subgroups.

In patients able to undergo strain analysis (n = 92), average GLS was –15.1%; 39 patients (42%) showed RELAPS value > 1; 82 (89%) patients had an SAB ratio > 2.1, and 39 (42%) had EFSR > 4.1. Figure 1B shows patient distribution according to these 3 LS-based indices.

No differences in clinical or demographic variables were found between the groups with RELAPS < 1 or > 1. The echocardiography variables showed that the RELAPS > 1 group had significantly more severe AS and increased LV hypertrophic remodeling. No differences were found in the conventional parameters used to evaluate systolic function; however, myocardial contraction fraction was significantly lower in the group with normal apical strain. No differences were found in diastolic function parameters.

In the multivariate analysis, predictive echocardiography variables for strain with an apical sparing pattern were LV mass (OR, 1.02; 95%CI, 1.01-1.03; *P* = .002), LV end-systolic volume (OR, 0.97; 95%CI, 0.94-0.99); *P* = .014), aortic valve area (OR, 0.10; 95%CI, 0.01-0.38; *P* = .018), and aortic ejection (OR, 0.98; 95%CI, 0.96-0.99; *P* = .010). The c-statistic was 85.6% (95%CI, 76.6%-94.7%).

In our series, patients with severe symptomatic AS without CA were highly likely to exhibit strain with an apical sparing phenotype and EFSR similar to that described in CA. These findings could have relevant clinical implications, as they would not be applicable in regular clinical practice for CA screening in patients with a condition as common as severe AS.

María Bastos Fernández,[a,b,c,*] Diego López Otero,[a,b,c] Javier López Pais,[a,b,c] Virginia Pubul Núñez,[b,d] Carmen Neiro Rey,[a,b] and José R. González-Juanatey[a,b,c]

[a]*Servicio de Cardiología, Hospital Clínico Universitario de Santiago, Santiago de Compostela, A Coruña, Spain*
[b]*Instituto para el Desarrollo e Integración de la Salud (IDIS), Santiago de Compostela, A Coruña, Spain*
[c]*Centro de Investigación Biomédica en Red de Enfermedades Cardiovasculares (CIBER-CV), Santiago de Compostela, A Coruña, Spain*
[d]*Servicio de Medicina Nuclear, Hospital Clínico Universitario de Santiago, Santiago de Compostela, A Coruña, Spain*

[*] Corresponding author:
E-mail address: bastosfernandez@yahoo.es
(M. Bastos Fernández).

Available online 4 July 2020

REFERENCES

1. Ternacle J, Krapf L, Mohty D, et al. Aortic stenosis and cardiac amyloidosis. *J Am Coll Cardiol.* 2019;74:2638–2651.
2. Phelan D, Collier P, Thavendiranathan P, et al. Relative apical sparing of longitudinal strain using two-dimensional speckle-tracking echocardiography is both sensitive and specific for the diagnosis of cardiac amyloidosis. *Heart.* 2012;98:1442–1448.
3. Liu D, Hu K, Niemann M, et al. Effect of combined systolic and diastolic functional parameter assessment for differentiation of cardiac amyloidosis from other causes of concentric left ventricular hypertrophy. *Circ Cardiovasc Imaging.* 2013;6:1066–1072.
4. Pagourelias ED, Mirea O, Duchenne J, et al. Echo parameters for differential diagnosis in cardiac amyloidosis. *Circ Cardiovasc Imaging.* 2017;10:e005588.

https://doi.org/10.1016/j.rec.2020.04.024
1885-5857/

Renin-angiotensin system blockers and outcomes during hydroxychloroquine treatment in patients hospitalized for COVID-19 pneumonia

Inhibidores del sistema renina-angiotensina y pronóstico durante tratamiento con hidroxicloroquina en pacientes hospitalizados por neumonía por COVID-19

To the Editor,

SARS-CoV infection requires virus binding to the membrane-bound form of angiotensin-converting enzyme 2 (ACE2). Hydroxychloroquine (HCQ) inhibits terminal glycosylation of ACE2 receptor, which may reduce the efficiency of its interaction with SARS-CoV spike protein.[1] Initial experiences during the COVID-19 pandemic supported the offlabel use of HCQ. However, its potential cardiotoxicity and still unclear benefit have eventually urged caution.[2]

High fatality rates have been reported in elderly individuals with COVID-19 and multiple cardiovascular comorbidities.[3] Concerns have arisen that angiotensin-converting enzyme inhibitors (ACEIs) and angiotensin receptor blockers (ARBs) might increase ACE2 receptor expression and patient susceptibility to viral entry into host cells, facilitating SARS-CoV-2 propagation.[4] Recent studies with different designs found no adverse effects associated with ACEIs/ARBs in various large populations with COVID-19 but did not report on HCQ coadministration.[5]